Indistinguishable single photons with flexible electronic triggering

optica

Indistinguishable single photons with flexible electronic triggering

Adetunmise C. Dada,[1,*] Ted S. Santana,[1] Ralph N. E. Malein,[1] Antonios Koutroumanis,[1] Yong Ma,[1,3] Joanna M. Zajac,[1] Ju Y. Lim,[2,4] Jin D. Song,[2] and Brian D. Gerardot[1]

[1]Institute for Photonics and Quantum Sciences, SUPA, Heriot-Watt University, Edinburgh EH14 4AS, UK
[2]Center for Opto-Electronic Convergence Systems, Korea Institute of Science and Technology, Seoul, South Korea
[3]Current address: Chongqing Institute of Green and Intelligent Technology, Chinese Academy of Sciences, Chongqing 400714, China
[4]Current address: Korea Photonics Technology Institute, Gwangju 61007, South Korea
*Corresponding author: a.c.dada@hw.ac.uk

A key ingredient for quantum photonic technologies is an on-demand source of indistinguishable single photons. State-of-the-art indistinguishable single-photon sources typically employ resonant excitation pulses with fixed repetition rates, creating a string of single photons with predetermined arrival times. However, in future applications, an independent electronic signal from a larger quantum circuit or network will trigger the generation of an indistinguishable photon. Further, operating the photon source up to the limit imposed by its lifetime is desirable. Here, we report on the application of a true on-demand approach in which we can electronically trigger the precise arrival time of a single photon as well as control the excitation pulse duration based on resonance fluorescence from a single InAs/GaAs quantum dot. We investigate in detail the effect of the finite duration of an excitation π pulse on the degree of photon antibunching. Finally, we demonstrate that highly indistinguishable single photons can be generated using this on-demand approach, enabling maximum flexibility for future applications.   © 2016 Optical Society of America

OCIS codes: (270.0270) Quantum optics; (250.5590) Quantum-well, -wire and -dot devices; (230.6080) Sources.

http://dx.doi.org/10.1364/OPTICA.3.000493

1. INTRODUCTION

Single photons remain prime candidates for realizing scalable schemes of quantum communication [1] and linear optical quantum computing [2,3]. The performance of such schemes relies critically on the indistinguishability of the single photons [4], in particular for key applications such as quantum repeaters [5] and boson sampling [6,7]. Of the various types of single-photon sources [8,9], semiconductor quantum dot (QD) systems are particularly promising for generating indistinguishable single photons because they offer a robust platform in which a single quantum system can be embedded within semiconductor devices and designed into bright single- and entangled-photon sources. The ideal single-photon source for quantum information processing (QIP) applications is one that generates a pure single-photon Fock state *on demand*, i.e., in response to an independent trigger signal from a user. Pulsed resonance fluorescence (RF) has been identified as the optimal way to deterministically generate high-quality photons with minimal dephasing. However, good-quality pulsed RF systems have so far utilized pulsed excitation generated by lasers with fixed repetition rates (~80 MHz) [10–15]. While this type of triggering could be said to be *deterministic*, it is not *on demand* since a user in this case has limited control over the excitation pulse arrival time and duration.

Here, we apply a flexible scheme for pulsed RF that triggers the generation of highly indistinguishable single photons such that a true on-demand operation is achieved via real-time electronic control. Our system uses a gigahertz-bandwidth electro-optic modulator (EOM) to modulate the output of a tunable continuous-wave (CW) laser for resonant excitation of a QD emitting at ~960 nm. In turn, the EOM is driven by a fast programmable electronic pulse-pattern generator (PPG). Such flexibility will greatly benefit the practical applications of single photons in quantum technologies.

Key performance measures for an on-demand single photon source include: the efficiency, defined as the probability of detecting a photon for a given electronic trigger; the purity, defined by the degree of antibunching as quantified by the second-order correlation function at zero delay; the degree of indistinguishability between individual photons as measured, e.g., by the Hong–Ou–Mandel (HOM)-type two-photon interference (TPI) visibility [16]; and crucially, the ability to determine or adjust, on demand, the timing and sequence of trigger pulses.

Considerable effort has been made toward realizing the on-demand triggering of single-photon generation by directly driving a QD electrically. Gigahertz-bandwidth electrical pulses (with pulse width $w > 270$ ps) have been used to rapidly modulate

the QD emission in resonant or non-resonant excitation [17–19]. Unfortunately, the single-photon purity in such hybrid schemes is less than ideal.

Similar effects have been observed when using an EOM to generate optical trigger pulses for a single-photon source (e.g., Ref. [20], $w = 500$ ps) where significant overlap between quantum dot RF pulses results in a quasi-CW stream of RF photons. EOM-generated optical pulses have been used for the direct detection of Rabi oscillations in QD excitons ($w = 2$ ns) [21], as well as fast triggering of single-photon generation with a large multi-photon contribution in the emission due to large trigger pulse widths ($w > 300$ ps) [22]. EOMs have also been applied for triggered photon generation from a QD using optical pulses with $w \geq 400$ ps specifically applied to QD spin manipulation and quantum teleportation [23]. Efforts have also been made to synchronously modulate QD photoluminescence generated using pulsed optical pumping with the goal of waveform shaping and temporal matching [24], as well as improved single-photon generation by filtering out multi-photon events and the incoherent portion of the photon wave packets [25]. The uses of EOMs for the modulation of single-photon wave packets generated in pulsed mode by non-QD sources have also been demonstrated [26,27].

In all these works, on-demand operation and pure single-photon generation of the sources have been undermined by high background counts and the widths of the excitation pulses. We use an EOM to demonstrate narrower optical-excitation-pulse widths and low background counts in the on-demand single-photon emission from a QD, better highlighting the potential of the flexible triggering for high-quality indistinguishable single-photon generation. We also exploit the flexibility of our setup for a detailed experimental study of the effect of the finite duration of excitation π pulses on the degree of photon antibunching.

2. METHODS

A. Sample Details

Our experiments were performed on self-assembled InGaAs quantum dots embedded in a GaAs Schottky diode for deterministic charge-state control. A broadband planar cavity antenna is used to enhance the photon extraction efficiency [28]. The QDs are at an antinode of a fifth-order planar cavity on top of an Au layer that functions simultaneously as a cavity mirror and Schottky gate. The simulations predict a photon extraction efficiency of ~27% into the first objective lens from this device.

B. Resonance Fluorescence System

We perform pulsed RF measurements on both the neutral exciton (X^0) and charged exciton states (X^{1-}) of a quantum dot. Our setup for triggering single-photon generation on demand is illustrated in Fig. 1(a). For RF, we use a cross-polarization technique in which orthogonally oriented linear polarizers are placed in the excitation and collection arms of a confocal microscope to suppress resonant-excitation-laser photons in the collected light [20], with extinction ratios of more than 10^7 in CW operation.

C. Pulsed Trigger Generation

We generate our optical excitation trigger signals using a programmable PPG that produces electronic pulses with widths of down to $w = 100$ ps at up to 3.35 GHz (period $T \simeq 300$ ps). Notably,

much faster pulses ($w < 30$ ps) can be achieved in the future with commercially available electronic pulse generators. The PPG drives a 20 Gb/s EOM, which in turn modulates the output of a resonant CW laser to obtain optical pulses that are practically identical to the driving electronic pulses with typical extinction ratios in excess of 30 dB. This extinction ratio is actively maintained by a modulator bias controller optoelectronic circuit through optical feedback. We are able to vary the pulse widths and repetition rates of the trigger pulses with high precision and also obtain optical pulses with user-defined bit-cycle data patterns.

D. Efficiencies

The efficiency of our microscope and detectors are as follows: the coupling of far-field radiation into a single-mode fiber: ~31.4%; linear polarizer: 43%; beam splitter surfaces: $(96\%)^4$; single-photon avalanche diode at $\lambda \sim 950$ nm: ~30%. The combination gives ~3.5%. The measured total efficiency of detecting a single photon per trigger pulse is ~0.36%. Based on this, we determine the photon extraction efficiency from the sample into the first lens to be ~10.4%.

3. RESULTS

Figure 1(a) illustrates our basic excitation and measurement setup. In Figs. 1(b) and 1(c), we respectively show time-resolved RF from the charged exciton states X^{1-} and X^0 following excitation with a π pulse ($w = 100$ ps), which gives exciton lifetimes of $T_1^{X1-} = 0.79 \pm 0.01$ ns and $T_1^{X0} = 0.78 \pm 0.02$ ns. The V-type energy structure of X^0 leads to quantum beats between the excited states (e.g., see Ref. [29]), which are directly detected here in the pulsed RF transient decay. The beat frequency corresponds to the fine-structure splitting (due to electron-hole exchange interaction) of $\delta_0 = 3.3$ GHz for this QD. In Fig. 1(d), we demonstrate the direct measurement of X^{1-} Rabi oscillations using 2 ns pulses from which we extract a dephasing time of $T_2 = 1.66 \pm 0.18$ ns using the lifetime of $T_1 = 0.79 \pm 0.01$ ns obtained from the measured X^{1-} decay with 100 ps pulses. This is consistent with the case of no pure dephasing where $T_2 = 2T_1$, confirming the absence of excitation-induced dephasing effects [30,31]. The first peak in the RF counts corresponds to a pulse area of π. We confirm the π-pulse area/power both using the direct measurement and by conventional methods (e.g., as used in Ref. [10]).

A. Antibunching and Efficiency

For our main autocorrelation measurements, we excite the quantum dot with 100 ps π pulses. Figure 2(a) shows a schematic of the Hanbury Brown and Twiss-type setup used in our antibunching measurements. In what follows, while we will use $g^2(\tau)$ to represent the autocorrelation function of the continuous time delay τ, $G^2(\tau_n)$ denotes the pulsed-mode autocorrelation function of the discretized time delay $\tau_n = nT$ obtained by integrating the nth pulse in $g^2(\tau)$, where $T = 1/f$ is the pulse period. In Fig. 2(b), we demonstrate antibunching at various trigger frequencies, as seen in the intensity-correlation histograms for the RF emission from the QD under pulsed excitation. Pulsed second-order correlations at zero delay $G^2(0)$ are calculated by integrating photon counts in the zero-time-delay peak and dividing by the average of the adjacent peaks over a range of ~650 ns around the time-zero peak, with standard deviations obtained
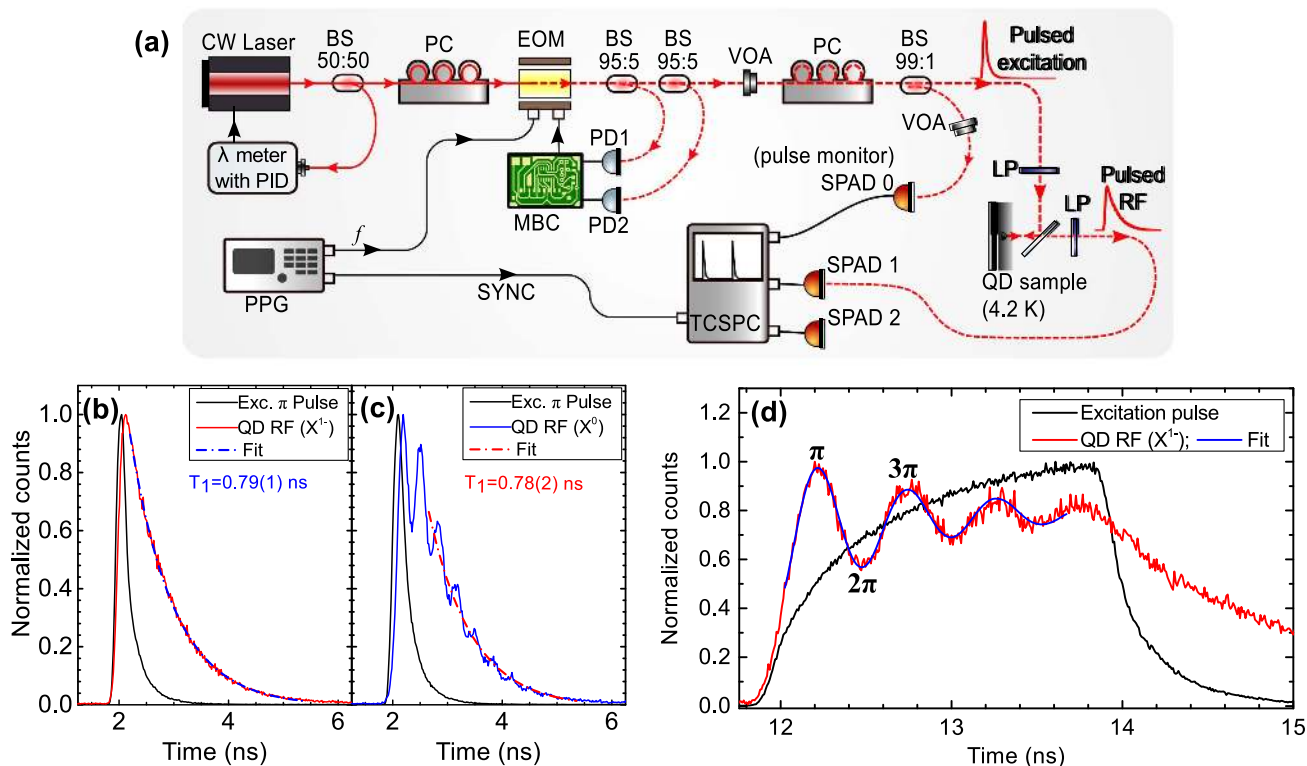
Fig. 1. (a) Flexibly triggered generation of resonance fluorescence from a quantum dot. We modulate the CW laser output using a 20 Gb/s EOM driven by a PPG capable of custom pulse patterns up to a frequency of $f = 3.35$ GHz. A modulator bias controller optoelectronic circuit maintains the high extinction ratio of the excitation pulses at >30 dB using a dual feedback system for increased dynamic range. BS, beam splitter; PC, polarization controller; VOA, variable optical attenuator; LP, linear polarizer; SPAD, single-photon avalanche diode. (b) and (c) Time-resolved QD resonance fluorescence under 100 ps π-pulse excitation. We overlay pulsed RF on a real-time measurement of the 100 ps excitation pulse (with spectral FWHM ~5.4 μeV, see Supplement 1) obtained by tapering off some of the power from the EOM output [see (a)]. A fit of a single exponential function to the exciton decay yields lifetimes of $T_1^{X1-} = 0.79(1)$ ns and $T_1^{X0} = 0.78(2)$ ns for X^{1-} and X^0, respectively. The V-type energy structure of X^0 leads to quantum beats between excited states, which are directly detected here in the pulsed RF transient decay. (d) Direct observation of Rabi oscillations in the charged exciton. A fit of the theoretical excited state population (see Supplement 1) to the Rabi oscillations gives a dephasing time $T_2 = (2.1 \pm 0.2) T_1$.
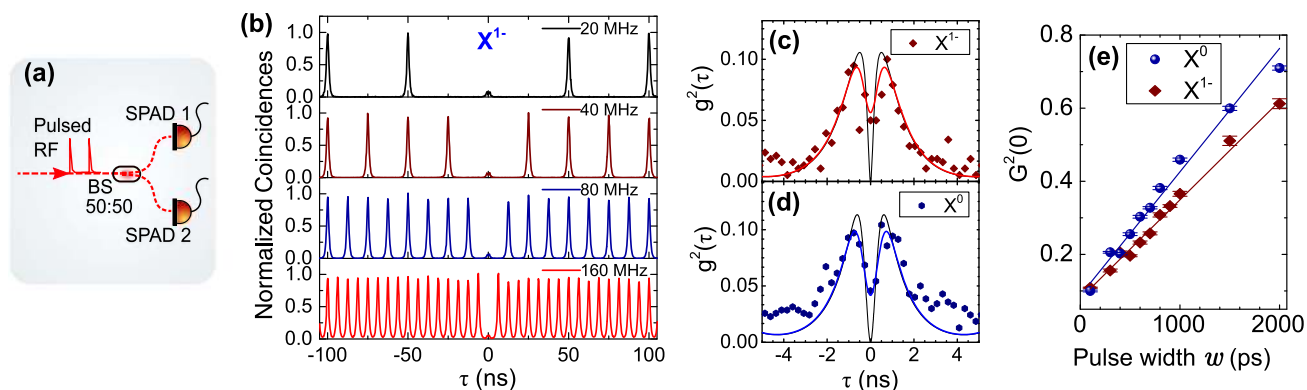

Fig. 2. Pulsed antibunching of on-demand triggered resonance-fluorescence photons. (a) Measurement setup. (b) Demonstration of flexible triggering of single-photon generation with examples at various frequencies. All measurements have a 180 s integration time. (c) and (d) show zoomed-in views of the time-zero peaks, revealing ideal antibunching smeared out by jitter in our detection system (FWHM ~150 ps). The data points represent raw experimental data, while the solid colored ($g^2(0) \simeq 0.05$) and black ($g^2(0) = 0.0$) lines, respectively, represent the results of quantum numerical simulation of the master equation (see Section SII of Supplement 1 for details) with and without convolution with the instrument response function of our detection system (FWHM ~150 ps). The pulsed antibunching is limited by the effect of the finite width of our excitation 100 ps pulses (the limit of our pulse generator) giving $G_{exp}^2(0) \simeq 0.1$ and $g_{exp}^2(0) \simeq 0.05$. (e) $G^2(0)$ as a function excitation pulse width under π-pulse excitation. Measurements were performed on both neutral and charged exciton states. The solid lines are linear fits to the experimental data.

from propagated Poissonian counting statistics of the raw counts. With 100 ps π pulses, we obtain the raw experimental values of $G^2(0) \sim 0.1$ and $g^2(0) \sim 0.05$, as shown in Figs. 2(c)–2(e). An increase in pulse widths leads to worse pulsed antibunching $G^2(0)$ [Fig. 2(e)], while the $g^2(0)$ values are unaffected.

We demonstrate the flexibility of the system and how it may be exploited to, e.g., maximize single-photon rates by performing autocorrelation measurements at varying repetition rates of 20–160 MHz and detect up to $\sim$0.45 MHz of single-photon counts (see Fig. 3). Also shown are the detected counts rates at saturation in the CW mode for each charge state. Peak coincidence counts of up to 5.5 K are measured at 160 MHz with a 256 ps time bin size in 180 s acquisitions. Beyond $\sim$160 MHz, the pulses in the RF autocorrelation function begin to overlap. This limit is imposed by the exciton lifetime. Single-photon count rates are obtained using the emission probability of more than one photon in a pulse, as obtained from the corresponding values of $G^2(0)$. From the count rates, we calculate the overall efficiency, i.e., the probability of detecting a pure single-photon state per trigger π-pulse to be $0.36 \pm 0.01\%$. Based on the combined efficiency of the collection optics and detectors ($\sim$3.5%, see Methods), we determine an extraction efficiency of $10.4 \pm 0.7\%$ into the first lens while the simulated extraction efficiency for our sample is $\sim$27% for a 0.68 NA objective lens (as used in our experiment) [28].

To reveal the nature of the non-ideal raw antibunching measured in our pulsed experiments and to verify the true quality of our single-photon source, we perform high timing resolution (jitter $\sim$150 ps) measurements of the intensity autocorrelation. Figures 2(c) and 2(d) show zoomed-in views of the small time-zero peaks for X^{1-} and X^0, which both reveal characteristic central dips. At zero delay, we see clear antibunching within the small peak with a vanishing raw multiphoton probability of $g^2(0) = 0.05$. To provide further insight, we use numerical simulations of the master equation for both X^0 and X^{1-} (at a magnetic field of $B_{ext} = 0$) as a V-type atomic system and a two-level system, respectively (see Section SII of the Supplement 1 for details). The small peaks surrounding $\tau = 0$ also manifest in the simulation results and are in good agreement with the experimental data,
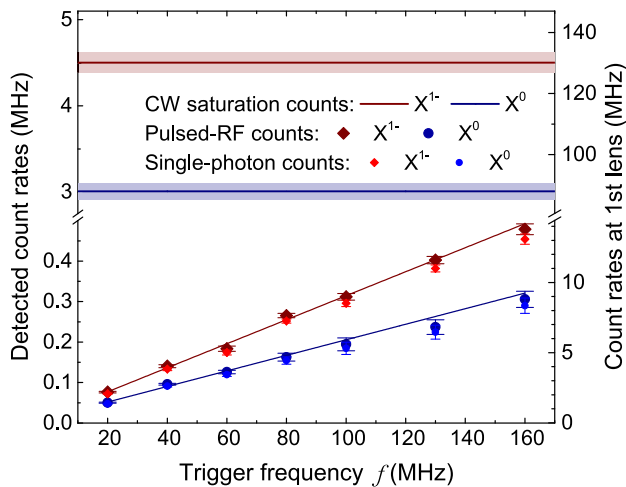
as shown in Figs. 2(c) and 2(d). The underlying mechanism of this non-ideality is a small probability to re-excite the system (following a first-photon emission event) within the pulse duration. The re-excitation probability increases with the pulse width, as confirmed in the simulation and experimentally [see Fig. 2(e)]. Importantly, the value of $g^2(0)$ is always zero at the middle of the time-zero peak, indicating that arbitrarily low $g^2(0)$ values can be achieved with shorter excitation pulses. Taking the instrument response function of our detection system into account, we estimate perfect antibunching ($g^2(0) = 0.0$). We conclude that although more than one photon may be emitted during the 100-ps-long excitation pulse with a small probability, these photons are not emitted at the same time.

B. Pulsed Two-Photon Interference

For TPI measurements, we send the QD photons into a HOM-type setup [see Fig. 4(a)] that consists of an unbalanced Mach–Zehnder (MZ) interferometer with a delay of $\Delta t = 49.70$ ns and polarization control in each arm to enable measurements with parallel ($\parallel$) and orthogonal ($\perp$) polarizations of interfering photons. The beam splitters in the MZ setup have nearly perfect 50:50 splitting ratios. We filter out the zero-phonon line from the most of the phonon sideband using a grating-based spectral filter (bandwidth $\Delta f = 12$ GHz and efficiency $\eta_f = 22\%$). Due to the flexibility of the trigger pulse generation, we are able to precisely match the repetition period of the pulses to Δt [see Fig. 4(b)] to obtain pulsed autocorrelation at a relative delay $T - \Delta t = 0$, shown in Figs. 4(c) and 4(d). The TPI visibility is defined as $v = [G^2_\perp(0) - G^2_\parallel(0)]/G^2_\perp(0)$. For X^0 and X^{1-}, we measure the raw visibilities of $v = 0.76 \pm 0.06$ and 0.28 ± 0.03, respectively. The raw indistinguishability of the X^0 photons is limited primarily by the multiphoton probability of $G^2(0) = 0.10 \pm 0.01$, which is in turn limited by the excitation pulse width as described above. When this is corrected for (by using $G'^2_\parallel(0) = G^2_\parallel(0) - G^2(0)$), we obtain TPI visibilities of $v = 0.96 \pm 0.06$ and 0.47 ± 0.03, respectively, for X^0 and X^{1-} without accounting for any other experimental imperfections. The reduced visibility of X^{1-} ($B_{ext} = 0$ T) is understood to be due to detuned Raman-scattered photons, which are distinguishable from both the elastic and incoherent components of the resonance fluorescence due to nuclear spin fluctuations (further details are provided in Ref. [32]). We stress that the Raman-scattered photons result in a total linewidth of less than 1 GHz, which is not filtered out by the 12 GHz-bandwidth spectral filter.

4. DISCUSSION

For on-demand single-photon sources to underpin scalable and efficient linear-optical quantum computing and networking, stringent criteria must be satisfied [33,34]. Our experimental results provide insight into the prospect of realizing the $G^2(0)$ requirements using resonance fluorescence-generated single photons. A crucial result is the effect of the pulse width relative to T_1 on $G^2(0)$. Typically, Purcell enhancement is considered desirable to reduce the impact of dephasing mechanisms [35–37] and enable increased clock rates. However, in pulsed RF, a faster T_1 also increases the probability for re-excitation given a certain excitation pulse width. We illustrate this trade-off using a numerical simulation for $G^2(0)$ as a function of the pulse width (Gaussian profile) for $T_1 = 250$ ps and 800 ps (Fig. 5). We see that in both cases, vanishing $G^2(0)$ can be obtained for ultra-short

Fig. 3. Count rates as a function of trigger pulse frequency. Raw experimental count rates on the detector are plotted for both X^0 and X^{1-}, as well as single-photon count rates, which are calculated from corresponding multiphoton probabilities [$G^2(0)$]. CW saturation counts are also shown for comparison.
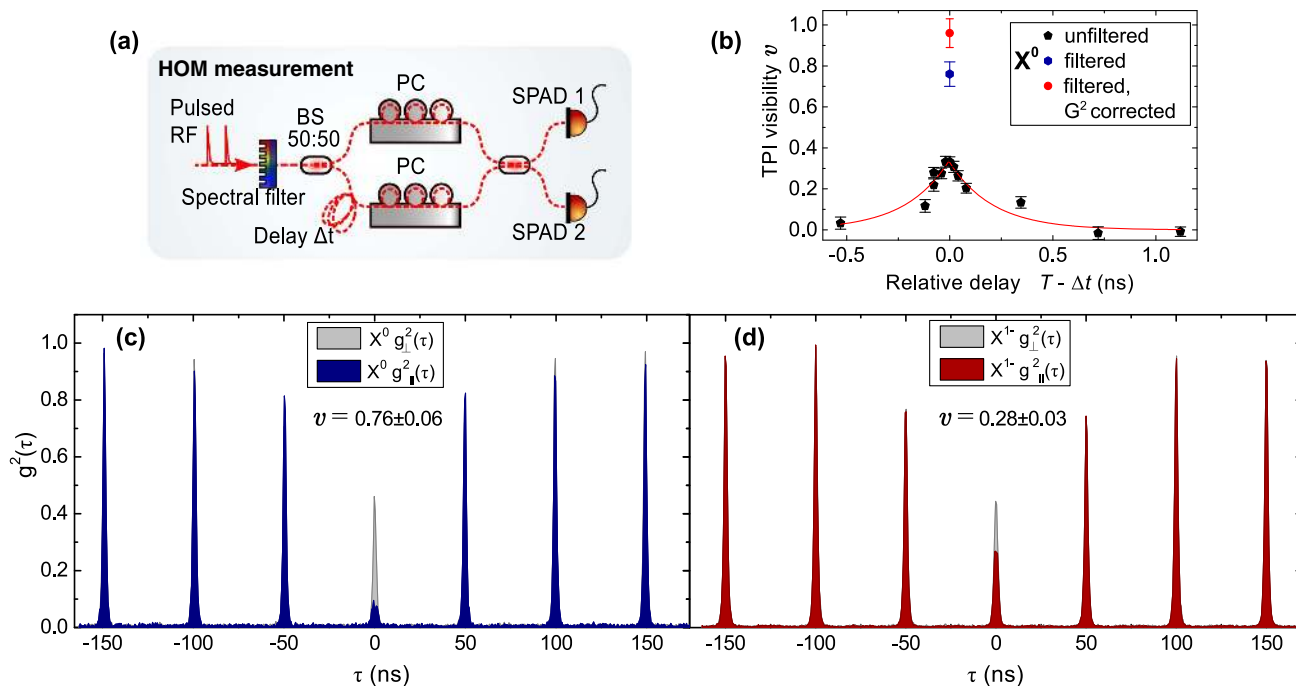
Fig. 4. Demonstration of indistinguishability of single photons triggered on demand. (a) HOM-type TPI results. The flexibility of our approach allows us to set the pulse period to match the delay in our HOM setup ($\Delta t = 49.7$ ns). (b) TPI visibility versus period. The measurements were performed on a neutral exciton line for X^0 using various pulse periods and hence delays between interfering photons with π-pulse excitation. TPI autocorrelation at zero relative delay. (c) shows results for X^0 photons and (d) for the charged exciton (X^{1-}), both at $B_{ext} = 0$ T. Measurements were performed using 100-ps-wide excitation pulses. The measurements plotted in gray are with orthogonal polarizations of interfering photons. (c) and (d) are measured with most of the phonon band filtered out using a grating-based spectral filter. The X^0 photons show TPI visibilities of $v = 0.76 \pm 0.06$ as raw experimental data and $v = 0.96 \pm 0.07$ when corrected *only* for multiphoton emission (G^2 corrected).

pulse widths, but practically, the minimization of $G^2(0)$ is best achieved with larger T_1 values. This is important for prospective applications (such as linear-optical QIP) of single photons generated using pulsed resonance fluorescence.

We have demonstrated flexible electronic triggering of on-demand single indistinguishable photons. This system offers several intriguing advantages for future applications. Whereas ultra-short excitation pulses lead to excitation-induced dephasing (EID) [31], coherent control with longer pulse durations is
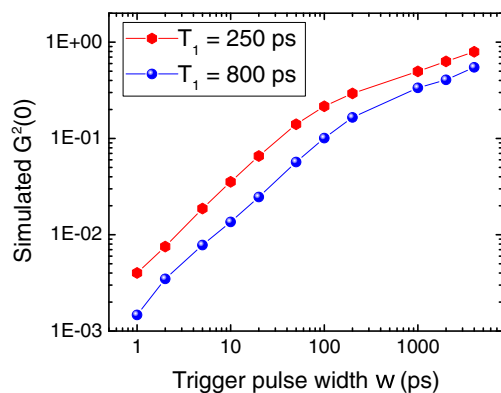

Fig. 5. Simulated $G^2(0)$ as a function of excitation pulse width under 0.81π-pulse excitation. Simulation of a two-level system with lifetimes of $T_1 = 800$ and 250 ps using a Gaussian (temporal) 0.81π-excitation pulse profiles with varying widths. We use 0.81π for the simulated Gaussian pulses because with a 100 ps width, they give the same $G^2(0)$ as the asymmetric 100 ps π pulses used in the experiment.

expected to minimize EID [38,39]. Hence, for some coherent control and read-out schemes, the flexibility of electronically tunable pulse durations is likely to be attractive. Another advantage of this approach is the possibility of specifically tailoring the pump pulses for quantum control processes such as stimulated Raman adiabatic passage [40] in quantum dots exhibiting spin-Lambda systems [41,42]. Finally, we note that the flexible technique presented here enables an excitation repetition rate up to the limit of that imposed by T_1, offering a significant boost in count rates for real applications. While overall system efficiencies need to be improved to realize an ideal single-photon source, recent developments in QIP protocols have made efficiency requirements considerably less stringent (e.g., in Ref. [33], efficient linear optical quantum computation is possible with an overall efficiency of 2/3), even as high-quality indistinguishability, antibunching, and brightness are now simultaneously being achieved (e.g., see Refs. [13–15]). The approach we demonstrate here is an important step toward combining these key performance features with true on-demand operation.

See Supplement 1 for supporting content.

REFERENCES

1. H. J. Kimble, "The quantum internet," Nature **453**, 1023–1030 (2008).

2. P. Kok, W. J. Munro, K. Nemoto, T. C. Ralph, J. P. Dowling, and G. J. Milburn, "Linear optical quantum computing with photonic qubits," Rev. Mod. Phys. **79**, 135–174 (2007).

3. J. L. O'Brien, A. Furusawa, and J. Vučković, "Photonic quantum technologies," Nat. Photonics **3**, 687–695 (2009).

4. P. P. Rohde and T. C. Ralph, "Error tolerance of the boson-sampling model for linear optics quantum computing," Phys. Rev. A **85**, 022332 (2012).

5. H. J. Briegel, W. Dur, J. I. Cirac, and P. Zoller, "Quantum repeaters: the role of imperfect local operations in quantum communication," Phys. Rev. Lett. **81**, 5932–5935 (1998).

6. J. B. Spring, B. J. Metcalf, P. C. Humphreys, W. S. Kolthammer, X.-M. Jin, M. Barbieri, A. Datta, N. Thomas-Peter, N. K. Langford, D. Kundys, J. C. Gates, B. J. Smith, P. G. R. Smith, and I. A. Walmsley, "Boson sampling on a photonic chip," Science **339**, 798–801 (2013).

7. M. A. Broome, A. Fedrizzi, S. Rahimi-Keshari, J. Dove, S. Aaronson, T. C. Ralph, and A. G. White, "Photonic boson sampling in a tunable circuit," Science **339**, 794–798 (2013).

8. B. Lounis and M. Orrit, "Single-photon sources," Rep. Prog. Phys. **68**, 1129–1179 (2005).

9. A. J. Shields, "Semiconductor quantum light sources," Nat. Photonics **1**, 215–223 (2007).

10. Y.-M. He, Y. He, Y.-J. Wei, D. Wu, M. Atature, C. Schneider, S. Höfling, M. Kamp, C.-Y. Lu, and J.-W. Pan, "On-demand semiconductor single-photon source with near-unity indistinguishability," Nat. Nanotechnol. **8**, 213–217 (2013).

11. M. Müller, S. Bounouar, K. D. Jöns, M. Glässl, and P. Michler, "On-demand generation of indistinguishable polarization-entangled photon pairs," Nat. Photonics **8**, 224–228 (2014).

12. T. Huber, A. Predojević, D. Föger, G. Solomon, and G. Weihs, "Optimal excitation conditions for indistinguishable photons from quantum dots," New J. Phys. **17**, 123025 (2015).

13. X. Ding, Y. He, Z. C. Duan, N. Gregersen, M. C. Chen, S. Unsleber, S. Maier, C. Schneider, M. Kamp, S. Höfling, C.-Y. Lu, and J.-W. Pan, "On-demand single photons with high extraction efficiency and near-unity indistinguishability from a resonantly driven quantum dot in a micropillar," Phys. Rev. Lett. **116**, 020401 (2016).

14. J. C. Loredo, N. A. Zakaria, N. Somaschi, C. Anton, L. D. Santis, V. Giesz, T. Grange, M. A. Broome, O. Gazzano, G. Coppola, I. Sagnes, A. Lemaitre, A. Auffeves, P. Senellart, M. P. Almeida, and A. G. White, "Scalable performance in solid-state single-photon sources," Optica **3**, 433–440 (2016).

15. N. Somaschi, V. Giesz, L. De Santis, J. C. Loredo, M. P. Almeida, G. Hornecker, S. L. Portalupi, T. Grange, C. Anton, J. Demory, C. Gomez, I. Sagnes, N. D. Lanzillotti-Kimura, A. Lemaître, A. Auffèves, A. G. White, L. Lanco, and P. Senellart, "Near-optimal single-photon sources in the solid state," Nat. Photonics **10**, 340–345 (2016).

16. C. K. Hong, Z. Y. Ou, and L. Mandel, "Measurement of subpicosecond time intervals between two photons by interference," Phys. Rev. Lett. **59**, 2044–2046 (1987).

17. J. H. Prechtel, P. A. Dalgarno, R. H. Hadfield, J. McFarlane, A. Badolato, P. M. Petroff, and R. J. Warburton, "Fast electro-optics of a single self-assembled quantum dot in a charge-tunable device," J. Appl. Phys. **111**, 043112 (2012).

18. Y. Cao, A. J. Bennett, D. J. P. Ellis, I. Farrer, D. A. Ritchie, and A. J. Shields, "Ultrafast electrical control of a resonantly driven single photon source," Appl. Phys. Lett. **105**, 051112 (2014).

19. A. Schlehahn, M. Gaafar, M. Vaupel, M. Gschrey, P. Schnauber, J. H. Schulze, S. Rodt, A. Strittmatter, W. Stolz, A. Rahimi-Iman, T. Heindel, M. Koch, and S. Reitzenstein, "Single-photon emission at a rate of 143 MHz from a deterministic quantum-dot microlens triggered by a mode-locked vertical-external-cavity surface-emitting laser," Appl. Phys. Lett. **107**, 041105 (2015).

20. C. Matthiesen, M. Geller, C. H. H. Schulte, C. Le Gall, J. Hansom, Z. Li, M. Hugues, E. Clarke, and M. Atature, "Phase-locked indistinguishable photons with synthesized waveforms from a solid-state source," Nat. Commun. **4**, 1600 (2013).

21. J. R. Schaibley, A. P. Burgers, G. A. McCracken, D. G. Steel, A. S. Bracker, D. Gammon, and L. J. Sham, "Direct detection of time-resolved Rabi oscillations in a single quantum dot via resonance fluorescence," Phys. Rev. B **87**, 115311 (2013).

22. K. Rivoire, S. Buckley, A. Majumdar, H. Kim, P. Petroff, and J. Vučković, "Fast quantum dot single photon source triggered at telecommunications wavelength," Appl. Phys. Lett. **98**, 083105 (2011).

23. W. Gao, P. Fallahi, E. Togan, A. Delteil, Y. Chin, J. Miguel-Sanchez, and A. Imamoğlu, "Quantum teleportation from a propagating photon to a solid-state spin qubit," Nat. Commun. **4**, 2744 (2013).

24. M. T. Rakher and K. Srinivasan, "Subnanosecond electro-optic modulation of triggered single photons from a quantum dot," Appl. Phys. Lett. **98**, 211103 (2011).

25. S. Ates, I. Agha, A. Gulinatti, I. Rech, A. Badolato, and K. Srinivasan, "Improving the performance of bright quantum dot single photon sources using temporal filtering via amplitude modulation," Sci. Rep. **3**, 1397 (2013).

26. P. Kolchin, C. Belthangady, S. Du, G. Yin, and S. Harris, "Electro-optic modulation of single photons," Phys. Rev. Lett. **101**, 103601 (2008).

27. H. P. Specht, J. Bochmann, M. Mücke, B. Weber, E. Figueroa, D. L. Moehring, and G. Rempe, "Phase shaping of single-photon wave packets," Nat. Photonics **3**, 469–472 (2009).

28. Y. Ma, P. E. Kremer, and B. D. Gerardot, "Efficient photon extraction from a quantum dot in a broad-band planar cavity antenna," J. Appl. Phys. **115**, 023106 (2014).

29. T. Flissikowski, A. Hundt, M. Lowisch, M. Rabe, and F. Henneberger, "Photon beats from a single semiconductor quantum dot," Phys. Rev. Lett. **86**, 3172–3175 (2001).

30. E. S. Kyoseva and N. V. Vitanov, "Resonant excitation amidst dephasing: an exact analytic solution," Phys. Rev. A **71**, 054102 (2005).

31. A. J. Ramsay, A. V. Gopal, E. M. Gauger, A. Nazir, B. W. Lovett, A. M. Fox, and M. S. Skolnick, "Damping of exciton Rabi rotations by acoustic phonons in optically excited InGaAs/GaAs quantum dots," Phys. Rev. Lett. **104**, 017402 (2010).

32. R. N. E. Malein, T. S. Santana, J. M. Zajac, A. C. Dada, E. M. Gauger, P. M. Petroff, J. Y. Lim, J. D. Song, and B. D. Gerardot, "Screening nuclear field fluctuations in quantum dots for indistinguishable photon generation," arXiv:1509.01057v1 (2015).

33. M. Varnava, D. E. Browne, and T. Rudolph, "How good must single photon sources and detectors be for efficient linear optical quantum computation?" Phys. Rev. Lett. **100**, 060502 (2008).

34. T. Jennewein, M. Barbieri, and A. G. White, "Single-photon device requirements for operating linear optics quantum computing outside the post-selection basis," J. Mod. Opt. **58**, 276–287 (2011).

35. C. Santori, D. Fattal, J. Vučković, G. S. Solomon, and Y. Yamamoto, "Indistinguishable photons from a single-photon device," Nature **419**, 594–597 (2002).

36. S. Laurent, S. Varoutsis, L. Le Gratiet, A. Lemaître, I. Sagnes, F. Raineri, A. Levenson, I. Robert-Philip, and I. Abram, "Indistinguishable single photons from a single-quantum dot in a two-dimensional photonic crystal cavity," Appl. Phys. Lett. **87**, 163107 (2005).

37. O. Gazzano, S. Michaelis de Vasconcellos, C. Arnold, A. Nowak, E. Galopin, I. Sagnes, L. Lanco, A. Lemaître, and P. Senellart, "Bright solid-state sources of indistinguishable single photons," Nat. Commun. **4**, 1425 (2013).

38. J. Förstner, C. Weber, J. Danckwerts, and A. Knorr, "Phonon-assisted damping of rabi oscillations in semiconductor quantum dots," Phys. Rev. Lett. **91**, 127401 (2003).

39. P. Machnikowski and L. Jacak, "Resonant nature of phonon-induced damping of Rabi oscillations in quantum dots," Phys. Rev. B **69**, 193302 (2004).

40. K. Bergmann, H. Theuer, and B. W. Shore, "Coherent population transfer among quantum states of atoms and molecules," Rev. Mod. Phys. **70**, 1003–1025 (1998).

41. X. Xu, Y. Wu, B. Sun, Q. Huang, J. Cheng, D. G. Steel, A. S. Bracker, D. Gammon, C. Emary, and L. J. Sham, "Fast spin state initialization in a singly charged InAs-GaAs quantum dot by optical cooling," Phys. Rev. Lett. **99**, 097401 (2007).

42. D. Brunner, B. D. Gerardot, P. A. Dalgarno, G. Wüst, K. Karrai, N. G. Stoltz, P. M. Petroff, and R. J. Warburton, "A coherent single-hole spin in a semiconductor," Science **325**, 70–72 (2009).